ISSN 1027-5495. Functional Materials, 29, No.4 (2022), p. 494-501.
doi:https://doi.org/10.15407/fm29.04.494

Optical spectroscopy of cyanine dyes *J*-aggregates in porous TiO_2 matrices

***I.Yu.Ropakova*[1], *P.V.Pisklova*[1], *I.I.Bespalova*[1], *I.A.Borovoy*[1], *O.G.Viagin*[1], *P.V.Mateychenko*[2], *S.L.Yefimova*[1], *A.V.Sorokin*[1]**

[1]Institute for Scintillation Materials, National Academy of Sciences of Ukraine, 60 Lenin Ave., 61001 Kharkiv, Ukraine
[2]Institute for Single Crystals, National Academy of Sciences of Ukraine, 60 Lenin Ave., 61001 Kharkiv, Ukraine

Received August 15, 2022

The features of the formation of three cyanine dyes *J*-aggregates in a porous TiO_2 matrix formed by positively charged microparticles were studied using optical spectroscopy. The formation of the *J*-aggregates was found to be better for cationic PIC and L-21 dyes compared to anionic BIC dye despite the charge of TiO_2 particles. This manifests itself both in the color of the matrices and in the spectral properties of *J*-aggregates. For all the dyes, the degree of aggregation was much lower than in solutions, and the monomers made a significant contribution to the absorption spectra. For *J*-aggregates in TiO_2 matrices, a weaker dipole-dipole interaction and a greater static disorder were found. Considering the spectral properties and stability, the PIC dye can be attributed to the best dye for the formation of *J*-aggregates in a porous TiO_2 matrix formed by microparticles.

Keywords: cyanine dye, *J*-aggregate, TiO_2 particle, porous matrix, luminescence, absorption.

Оптична спектроскопія *J*-агрегатів ціанінових барвників у пористих матрицях TiO_2.
І.Ю.Ропакова, П.В.Пісклова, І.І.Беспалова, І.А.Боровой, О.Г.Вягін, П.В.Матейченко, С.Л.Єфімова, А.В.Сорокін

Методами оптичної спектроскопії досліджено особливості формування *J*-агрегатів трьох ціанінових барвників у пористій матриці TiO_2, утвореній позитивно зарядженими мікрочастинками. Було виявлено краще утворення *J*-агрегатів для катіонних барвників PIC і L-21 порівняно з аніонним барвником BIC, незважаючи на заряд частинок TiO_2. Це проявляється як у забарвленні матриць, так і в спектральних властивостях *J*-агрегатів. Для всіх барвників ступінь агрегації був значно меншим, ніж у розчинах, і мономери давали значний внесок у спектри поглинання. Для *J*-агрегатів у матрицях TiO_2 виявлено слабшу диполь-дипольну взаємодію та більший статичний безлад. Враховуючи спектральні властивості та стабільність, можна назвати барвник PIC найкращим випадком формування *J*-агрегатів у пористій матриці TiO_2, утвореній мікрочастинками.

1. Introduction

Molecules of some organic dyes and pigments, such as cyanines, merocyanines, squaraines, etc., show a unique ability to associate; as a result, various compositions and structures from dimers to supramolecular systems can form in solutions or on the surface of aggregates [1]. Particular attention is paid to *J*-aggregates, which have an ordered structure and specific spectral properties [2–7]. High-molecular ordered aggregates, called *J*-aggregates, are low-dimensional crystals, the optical properties of which are due to the delocalization of electronic excitations in some areas with the formation of Frenkel excitons [2–7]. Depending on the molecular arrangement, the

excitonic band can be narrow, red-shifted (called the J-band), or broad, blue-shifted (called the H-band)[2–7]. Due to the excitonic nature of optical properties and their strong dependence on the structure, J-aggregates reveal many unique spectral characteristics, such as a very narrow J-band (with the width depending on the exciton coherence length), a large excitonic band shift, near-resonance fluorescence, giant cubic susceptibility, exciton superradiance, a very high oscillator strength, etc.[2–7]. J-aggregates typically form in highly concentrated solutions and have a structure that is intermediate between amorphous and crystalline. In solutions, J-aggregates are usually linear or closed molecular chains capable of forming complex supramolecular structures[2–7].

Aggregation processes and unique optical properties of dye molecular aggregates attract great interest both for basic research and in the applied aspect[1–9]. New promising applications of J-aggregates for the development of new generation LED devices, frequency conversion of laser radiation, creation of photovoltaic devices based on molecular units, etc. have been proposed [2, 7, 10–14]. For practical applications, J-aggregates in the form of solid-state samples are more promising than solutions due to higher stability [2–7]. Unfortunately, J-aggregates can change their structure in solid nanostructured materials, such as nanoporous matrices or polymer films, causing a modification of spectral properties [2–7]. For example, we reported a change in the optical properties of BIC, PIC, amphi-PIC, and TDBC J-aggregates when formed in nanostructured media, such as polymer films and nanoporous AAO matrices [15–18].

Porous titanium dioxide is an attractive material due to its high stability, superior electron transport properties, and the facilities to control the surface morphology[19–21]. Thus, it finds multiple applications, first of all, in organic photovoltaics and perovskite solar cells[19–21]. It was shown that cyanine dyes are efficiently adsorbed on TiO_2 surfaces as monomers or J-aggregates and can be used as photosensitizers for organic solar cells or photodetectors[11, 12, 22–26]. Mostly, the anionic cyanine dyes were utilized to be adsorbed on positively charged TiO_2 surfaces in these studies.

In this work, we present the results of J-aggregation of cationic dyes PIC and L-21 and anionic dye BIC in highly porous TiO_2 matrices formed using TiO_2 microparticles.

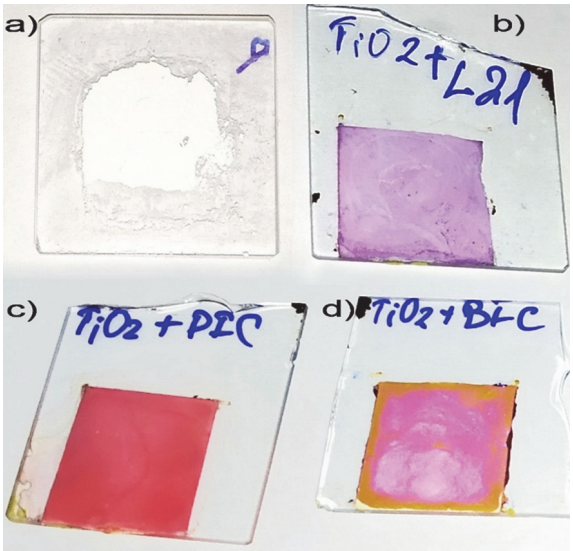

Fig. 1. Photographic images of TiO_2 matrices colored by J-aggregates of different dyes: a) pure matrix, b) L-21, c) PIC, and d) BIC.

2. Experimental

TiO_2 microparticles were formed as follows: 10 ml of titanium (IV) butoxide (Sigma Aldrich, USA) was added to 10 ml of butanol, and this mixture was stirred until a homogeneous solution was obtained; then an aqueous surfactant solution (0.2 ml of OP-9 in 10 ml of H_2O) was added dropwise with vigorous stirring. As a result, a suspension of amorphous TiO_2 in an aqueous butanol solution was obtained. This suspension was heated to 80°C for the time required to obtain a "paste" of amorphous TiO_2. Then the "paste" was heated to 150°C and kept for 2 hours. The resulting amorphous TiO_2 powder was annealed at 300°C for 12 hours. Thus, a fine powder of TiO_2 particles was obtained. An aqueous solution of acetic acid (10 % wt.) was added to the obtained fine powder. This mixture was stirred to form a homogeneous white paste. Next, this paste was applied to the glass substrate in the form of a thin layer with a thickness of approximately 100 μm and annealed at a temperature of 350°C for 30 minutes. The color of the TiO_2 microporous film changed from white to light brown, and then again to white (Fig. 1a), which indicated the annealing of the organic part of the film (i.e., solvent).

PIC (1,1′-diethyl-2,2′-cyanine iodide, pseudoisocyanine, Fig. 2a) dye was purchased from Sigma Aldrich (USA) and used as received. PIC J-aggregates were prepared by dissolving the PIC (0.5 mM) in an aque-

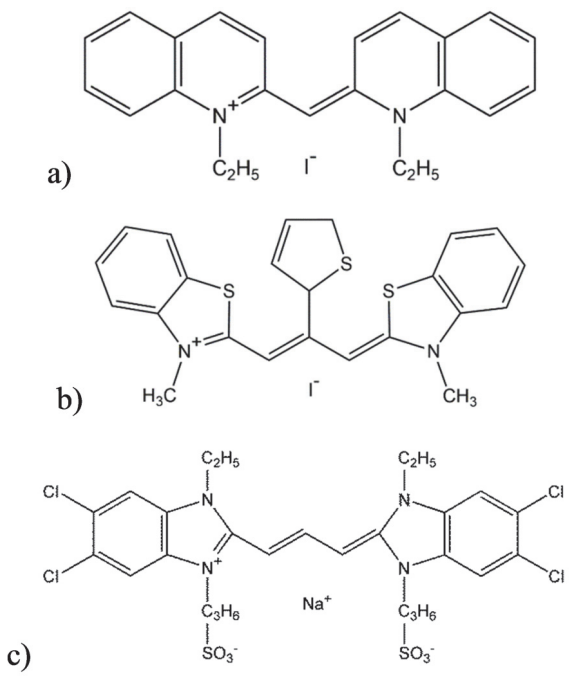

Fig. 2. Structural formula of the dyes: a) PIC, b) L-21, and c) BIC.

ous NaCl (0.2 M) solution under moderate heating (< 80°C). Then the solution was slowly cooled down to room temperature. L-21 (3,3′-dimethyl-9-thienyl-thiacarbocyanine iodide, Fig. 2b) dye was purchased from Otava Ltd (Ukraine) and used as received. L-21 *J*-aggregates were prepared from a stock solution of the dye in DMF (2 mM) by its dilution with deionized water at the ratio of 1:9 providing a 0.2 mM dye concentration in the final solution. BIC dye (1,1′-disulfopropyl-3,3′-diethyl-5,5′,6,6′-tetrachl oro-benzimidazolylcarbocyanine sodium salt, Fig. 2c) was synthesized by Dr.I.A.Borovoy with purity controlled by NMR and thin layer chromatography. BIC *J*-aggregates were prepared by dilution in deionized water to get a 1 mM dye concentration.

To inject the *J*-aggregates into the TiO_2 matrix, it was immersed in the *J*-aggregates aqueous solutions for at least 2 hours, which resulted in intense uniform coloring of the matrix. Then the surface of the sample was washed with water to remove the dye excess and blow-dried at room temperature. As a result, intensively colored films were obtained (Fig. 1).

Measurements of absorption spectra were performed using a two-beam spectrophotometer SPECORD 200 (Analytik Jena, Germany). To measure the absorption spectra of opaque dye samples in TiO_2 films, a fluorescent microscope was used in a transmitted light mode with a 10X/0.50NA objective and supplied by a spectrophotometer USB4000 (Ocean Optics, USA). A Lumina spectrofluorimeter (ThermoScientific, USA) was used to study the luminescent properties of cyanine dye *J*-aggregates, namely, to measure stationary spectra of luminescence and luminescence excitation. Luminescence decay curves were measured using a Fluotime 200 picosecond spectrofluorimeter (PicoQuant, Germany) using picosecond laser modules with radiation wavelengths of 439 nm and 531 nm. HQ460LP and HQ560LP filters (Chroma, USA) were used to ensure a high-quality emission analysis. Electron microscopy images of the films were obtained by applying them to a graphite substrate; a scanning electron microscope (SEM) JSM-6390LV (JEOL Company, USA) at a voltage of 15 kV was used.

Microscopic images of the TiO_2 matrix obtained using a scanning electron microscope (SEM) showed that it is the sintered highly porous microscopic particles of different sizes (Fig. 3). Typically, the microparticles of TiO_2 prepared by the chosen method are positively charged [19–21]. The high porosity of the obtained TiO_2 matrix provides effective adsorption of organic dyes, which is confirmed by the coloration of the matrices with *J*-aggregates of PIC, L-21, and BIC (Fig. 1).

3. Results and discussion

3.1. PIC J-aggregates. *J*-aggregates of PIC dye may be among the most studied aggregates of cyanine dyes[2–7]. In aqueous solutions, they exhibit a very narrow *J*-band simultaneously with a high fluorescence intensity, which indicates a very high degree of order within the molecular chain and a filamentous quasi-one-dimensional structure[2–7]. However, their formation in solid or nanostructured media can lead to a change in the *J*-aggregate structure and, hence, their optical properties[7, 17, 18]. Due to this effect, one can use PIC *J*-aggregates as a fluorescence probe to study the features of aggregation in various media or on various surfaces.

In an aqueous electrolyte solution, PIC *J*-aggregates exhibit three absorption bands (Fig. 4a, curve *1′*): an *H*-band (λ_{max} = 492 nm), a monomer band (λ_{max} = 525 nm) and a very narrow *J*-band (λ_{max} = 573.5 nm, $\Delta\nu_{FWHM}$ = 180 cm^{-1}). In the luminescence spectrum (Fig. 4a, curve *2′*),

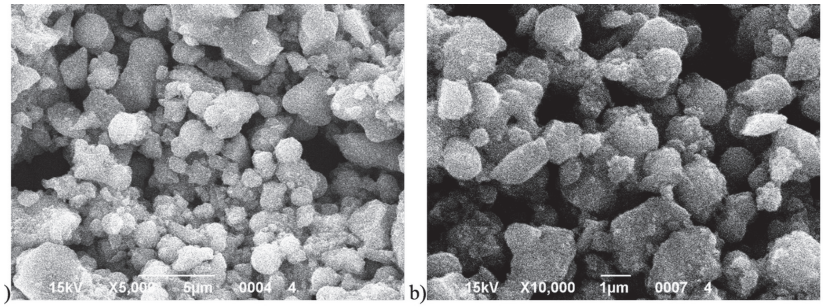

Fig. 3. SEM images of TiO_2 matrices with different resolutions.

only a narrow resonant intense band (λ_{max} = 574 nm, $\Delta\nu_{Stokes}$ = 15 cm^{-1}) can be observed. That is typical for PIC *J*-aggregates, since the monomers do not emit in solutions due to the *cis-trans* isomerization effect, while in aggregates with both *H*- and *J*-bands, only low energy excitonic states (corresponding to *J*-band) emit radiation[2—7].

The porous TiO_2 matrix turned out to be well colored after immersing in a solution of PIC *J*-aggregates, indicating effective PIC dye adsorption on the matrix surfaces despite the same charge of the TiO_2 surface and dye molecules (Fig. 1c). Possibly, the Coulomb repulsion is partially blocked by NaCl salt ions presented in the solution of *J*-aggregates. In addition, it is necessary to take into account the hydrophobic interaction, which significantly affects the behavior of cyanine dyes upon aggregation [2–7, 22].

As can be seen from the absorption spectra (Fig. 4a, curve 1), the aggregation degree of PIC dye is lower than in the solution (Fig. 4a, curve 1′), and, consequently, the exciton bands (the *H*-band with $\lambda_{max}^{TiO_2}$ = 487 nm and the *J*-band with $\lambda_{max}^{TiO_2}$ = 567 nm) are less intense relative to the monomer band ($\lambda_{max}^{TiO_2}$ = 523 nm). Indeed, such a weaker aggregation can be expected taking into account the Coulomb repulsion between the dye and TiO_2 particles. Nevertheless, the *J*-band is still resolved in the absorption spectrum (Fig. 4a, curve 1). One can see that all bands of the PIC *J*-aggregates are slightly shifted to the blue spectral region compared to the ones in the solution. The spectral shift for monomer and exciton bands has a different nature. While the shift of the monomer band is associated with the changes in its solvate shell (so-called solvatochromic effect [27, 28]), the shift of exciton bands is due to changing the dipole-dipole strength *J*, which can be found as[29]:

$$J = \frac{\nu_{mon} - \nu_J}{2.4}, \quad (1)$$

where ν_{mon} and ν_J are maxima of the monomer band and the *J*-band expressed in cm^{-1}, respectively. The strength of the dipole-dipole interaction can be estimated for PIC *J*-aggregates in the solution as J_{sol} ~ 670 cm^{-1}, and in the TiO_2 matrix — as J_{TiO2} ~ 620 cm^{-1}. Thus, the dipole-dipole interaction is weaker for PIC *J*-aggregates in the TiO_2 matrix compared to those in the solution.

In the luminescence spectrum (Fig. 4a, curve 2), only one wide low-intense band was found with $\lambda_{max}^{TiO_2}$ = 590 nm, which can be attributed to the emission of the aggregate, since in the solid samples, the emission of the monomer exhibits the band maximum at a shorter wavelength[7]. The high width of the luminescence band of the *J*-aggregate with a large Stokes shift of the band ($\Delta\nu_{Stokes}^{TiO_2}$ = 685 cm^{-1}) indicates a significant localization and self-trapping of excitons in the *J*-aggregates[7, 18]. Typically, such an effect is caused by a significant disorder in the aggregate structure due to an inhomogeneous micro-environment of *J*-aggregates[7].

To estimate the static disorder in the *J*-aggregate structure one needs to estimate an exciton coherence length, which is one of the most important parameters showing the spreading of the exciton state over molecular chains[2–7]. We can estimate the exciton coherence length from the experimental data using[7]:

$$N_{coh} = \frac{3 \cdot (\Delta\nu_{FWHM}^{mon})^2}{2 \cdot (\Delta\nu_{FWHM}^{J})^2} - 1, \quad (2)$$

where $\Delta\nu_{FWHM}^{mon}$ and $\Delta\nu_{FWHM}^{J}$ are full widths at half maximum of the monomer and *J*-bands, respectively. For PIC *J*-aggregates in the solution, the N_{coh} is approximately 45,

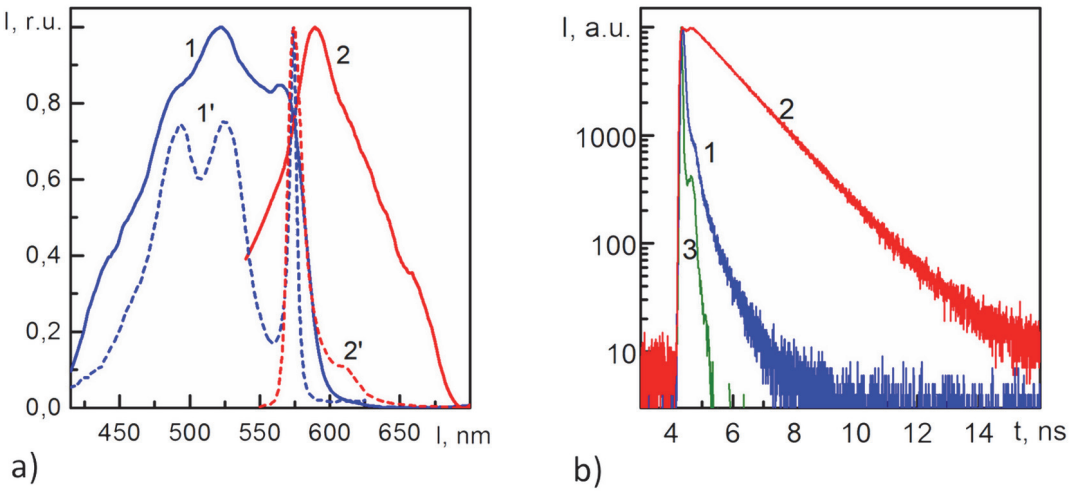

Fig. 4. a) Absorption (curves 1) and luminescence (curves 2, λ_{exc} = 530 nm) spectra of PIC *J*-aggregates in the TiO_2 matrix (curves 1 and 2) and aqueous solution (curves 1′ and 2′), the spectra are normalized for clarity; b) luminescence (λ_{exc} = 531 nm) decay for PIC *J*-aggregates in TiO_2 matrix (curve 1, λ_{reg} = 590 nm) and aqueous solution (curve 2, λ_{reg} = 575 nm), curve 3 — IRF.

taking into account the width of the monomer ~ 990 cm^{-1} and the width of the *J*-band ~ 130 cm^{-1}[18]. For PIC *J*-aggregates in the microporous matrix, the width of the *J*-band can be estimated by subtraction of the band of the monomer from the whole spectrum, and we obtain $\Delta\nu_{FWHM}^{TiO_2}$ ~ 980 cm^{-1} (Fig. 4a, curve 1). Hence, the exciton coherence length $N_{coh}^{TiO_2}$ is only ~ 2, taking into account the wider the band of the monomer in the solid sample[18]. The significantly shorter exciton coherence length for PIC *J*-aggregates in the TiO_2 matrix compared to the solution case confirms the large static disorder in the PIC *J*-aggregates formed in the TiO_2 matrix.

Thus, we can conclude that, despite the same charge of the dye and matrix, PIC *J*-aggregates still form on the microporous surface. However, the aggregation degree is small and the *J*-aggregates exhibit a very large static disorder leading to exciton localization and self-trapping. As a result, the luminescence yield of the *J*-aggregate is strongly quenched, which manifests itself not only in a low luminescence intensity (Fig. 4a, curve *2*) but also in a much shorter luminescence decay curve for the *J*-aggregates in the TiO_2 matrix (Fig. 4b, curve *1*).

Indeed, in the aqueous solution, the exponential luminescence decay was obtained for PIC *J*-aggregates with a lifetime τ ~ 1.39 ns (Fig. 4b, curve 2) [30]. However, in the TiO_2 matrix, the luminescence decay curve is non-exponential and can be described by three exponents with τ_1 ~ 75 ps (79 %), τ_2 ~ 320 ps (17 %), and τ_3 ~ 800 ps (4 %), which provides the average lifetime τ_{av} ~ 150 ps taking into account fractional amplitudes. The lifetime shortening due to the luminescence quenching is typical for *J*-aggregates formed in solid media[7]. However, for PIC *J*-aggregates formed in layered polymer films, we obtained the average lifetime τ_{av} ~ 40 ps and the luminescence quantum yield η ~ 0.5 % [30]; while in the TiO_2 matrix, the average lifetime (τ_{av} ~ 150 ps) turned out to be 3 times longer, whereas the luminescence quantum yield is comparable with that in the polymer film and maybe even less (wasn't measured due to too weak yield). It can be assumed, that an additional contribution to luminescence quenching is made by electron transfer from PIC *J*-aggregates to TiO_2 particles[31].

3.2. L-21 J-aggregates. Another cationic dye, for which *J*-aggregation in a TiO_2 porous matrix was studied, is L-21 (Fig. 2b). The L-21 *J*-aggregates were previously investigated in aqueous solutions under interaction with nucleic acids[32], surfactant micelles[33] and inorganic nanoparticles[34]. The features of the exciton structure of an L-21 *J*-aggregate are the presence of both *H*- and *J*-bands, the former being much more intense than the latter, and a quite large spectral shift of the *J*-band relative to the monomer band (Fig.

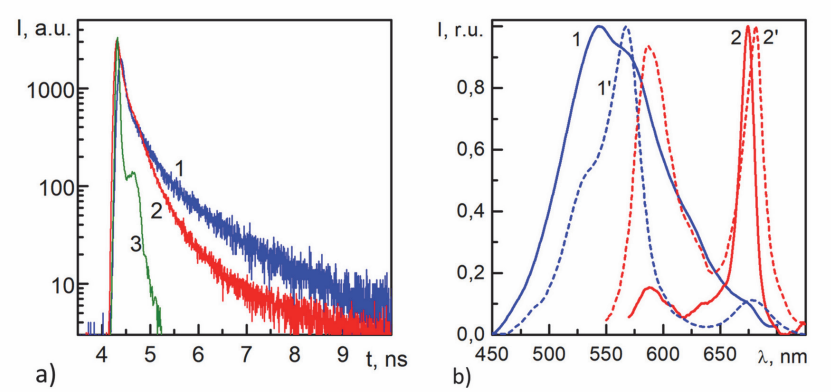

Fig. 5. a) Absorption (curves 1) and luminescence (curves 2, λ_{exc} = 530 nm) spectra of L-21 *J*-aggregates in the TiO_2 matrix (curves 1 and 2) and aqueous solution (curves 1′ and 2′), the spectra are normalized for clarity; b) luminescence (λ_{exc} = 531 nm) decay for L-21 *J*-aggregates in the TiO_2 matrix (curve 1, λ_{reg} = 675 nm) and aqueous solution (curve 2, λ_{reg} = 681 nm), curve 3 — IRF.

5a)[32–34]. In the binary solution DMF:water (1:9), L-21 dye typically demonstrates low aggregation, and the monomer band (λ_{max} = 567.5 nm) is dominated in the absorption spectrum (Fig. 5a, curve *1′*); while the *J*-aggregates exhibit only a very wide and low-intense *J*-band ($\Delta\nu_{FWHM}$ ~ 845 cm^{-1}, λ_{max} = 678 nm). According to Eq. (1), we can estimate the dipole-dipole interaction as J_{sol} ~ 1195 cm^{-1}, which is about twice as large as for PIC *J*-aggregates (Fig. 4a). Such a large difference can be associated with the specific structure of L-21 dye (Fig. 2b), namely, the three-methine "bridge" and the 9-thienyl central radical, which provide a much larger dipole moment of the optical transition in the dye. As the monomer band width is only ~ 770 cm^{-1}, there is no possibility to estimate the exciton coherence length according to Eq. (2). In the luminescence spectrum of L-21 dye in the binary solution, two bands can be resolved, namely, the monomer band (λ_{max} = 588 nm) and the exciton band (λ_{max} = 681 nm, $\Delta\nu_{Stokes}$ = 65 cm^{-1}) which is narrower and a bit more intense than the monomer luminescence (Fig. 5a, curve 2′). The relatively narrow luminescence band of L-21 *J*-aggregates with a very small Stokes shift is an indication that the large width of the *J*-band is due to the inhomogeneity of the distribution of aggregates rather than a large static disorder. Similar to PIC *J*-aggregates, despite the same charge of TiO_2 particles and the dye, L-21 *J*-aggregates color the matrix relatively homogeneously (Fig. 1b), although the colors differ due to the different spectral positions of the monomer and exciton bands for PIC and L-21 *J*-aggregates. As in the case of interaction with different nanoparticles in solutions[32–34], adsorption on the TiO_2 surface leads to spectral changes for L-21 *J*-aggregates (Fig. 5a, curves 2). In the absorption spectrum (Fig. 5a, curve 1), two additional bands appear, one of which is the *H*-band (λ_{max} = 544 nm) and the second one seen as a shoulder (λ_{max} = 625 nm) is the band of *J*-dimers[32]. The *J*-band (λ_{max} = 674 nm) appears to be slightly blue-shifted and much less resolved compared to the solution case, but much narrower ($\Delta\nu_{FWHM}$ ~ 490 cm^{-1}). According to equations (1) and (2), we obtain J_{TiO2} ~ 1160 cm^{-1} and N_{coh} ~ 3, respectively. Thus, we can conclude that the L-21 *J*-aggregates in the TiO_2 matrix exhibit a weaker dipole-dipole interaction and a small exciton coherence length, which indicates hindered aggregation on the TiO_2 surface, as expected due to the Coulomb repulsion. The general form of the absorption spectrum of the L-21 *J*-aggregates in the TiO_2 matrix is very similar to that in the interaction with RNA, where in contrast to the DNA surface, much fewer suitable regions for extended aggregation were assumed [32].

Despite the restricted L-21 aggregation in the TiO_2 matrix, the luminescence band of the aggregates (λ_{max} = 674.5 nm, $\Delta\nu_{Stokes}$ = 10 cm^{-1}) is much more intense compared to the monomer emission (λ_{max} = 588 nm) (Fig. 5a, curve 2). Interestingly, there is no spectral shift for both absorption and emission of the monomer in the TiO_2 matrix with respect to the solution (Fig. 5a). If we compare the luminescence

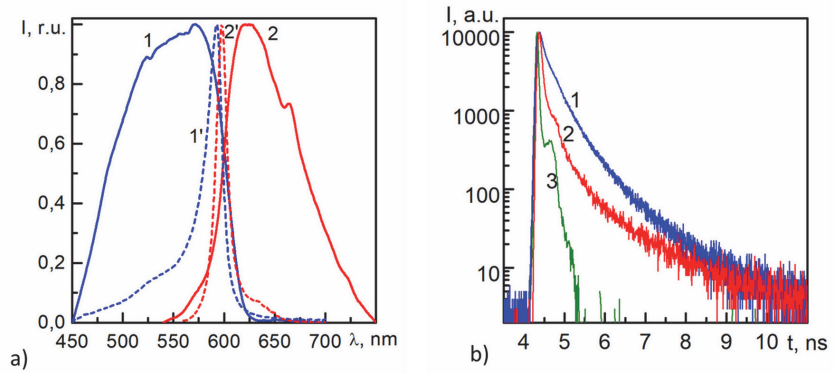

Fig. 6. a) Absorption (curves 1) and luminescence (curves 2, λ_{exc} = 530 nm) spectra of BIC *J*-aggregates in TiO_2 matrix (curves 1 and 2) and aqueous solution (curves 1′ and 2′) the spectra are normalized for clarity; b) luminescence (λ_{exc} = 531 nm) decay for BIC *J*-aggregates in the TiO_2 matrix (curve 1, λ_{reg} = 630 nm) and aqueous solution (curve 2, λ_{reg} = 600 nm), curve 3 — IRF.

decay of L-21 *J*-aggregates in the TiO_2 matrix (Fig. 5b, curve 1) and in the solution (Fig. 5b, curve 2), we can find that they are quite similar, with a longer lifetime in the matrix (τ_{av} ~ 210 ps) compared to one in the solution (τ_{av} ~ 150 ps).

Therefore, we can conclude that despite the Coulomb repulsion between TiO_2 particles and dye, which leads to restricted L-21 aggregation in the TiO_2 matrix, the *J*-aggregates of L-21 demonstrate improved spectral properties when adsorbed on the TiO_2 surface compared to those in the solution, although worse than when interacting with some nanoparticles[32–34]. Unfortunately, the L-21 *J*-aggregates show very low stability when adsorbing on the TiO_2 surface, and a strongly colored matrix like that shown in Fig. 1b turned out to be almost colorless the very next day after sample preparation.

3.3. BIC J-aggregates. The third dye, which *J*-aggregates were studied in this research, is the anionic dye BIC (Fig. 2c). The spectral properties of the BIC *J*-aggregate are well studied[2, 7, 15, 35] including those for the *J*-aggregates in the anodic aluminum oxide (AAO) porous matrix[17]. Since the BIC dye is an anionic one, we expected the similarity of the properties of the *J*-aggregates in the TiO_2 matrix to those in water. Surprisingly, in contrast to the PIC and L-21 *J*-aggregates, the TiO_2 matrix appeared to be very inhomogeneously colored by BIC *J*-aggregates, with most of the dye concentrated along the matrix boundary (Fig. 1d). Moreover, the absorption and luminescence spectra of the BIC *J*-aggregates in the TiO_2 matrix significantly differed from those in water (Fig. 6a). Indeed, the absorption spectrum of the BIC *J*-aggregates in water demonstrated (Fig. 6a, curve 1′) a single intense narrow *J*-band ($\Delta\nu_{FWHM}$ ~ 560 cm^{-1}, λ_{max} = 592.5 nm) together with the low-intense monomer band (λ_{max} = 530 nm); while the luminescence spectrum showed only one narrow intense band (λ_{max} = 674.5 nm, $\Delta\nu_{Stokes}$ = 10 cm^{-1}) corresponding to the emission of the aggregate (Fig. 6a, curve 2′). On the contrary, the BIC *J*-aggregates in the TiO_2 matrix exhibited a very wide absorption band (Fig. 6a, curve 1) with some features which can presumably be attributed to the *H*-band (λ_{max} ~ 485 nm) and the *J*-band (λ_{max} = 571 nm), which contributed to the monomer band (λ_{max} = 530 nm). Similarly, in the luminescence spectrum (Fig. 6a, curve 2′), one can also find a very wide low-intense emission band (λ_{max} = 623 nm, $\Delta\nu_{Stokes}$ = 1465 cm^{-1}). It is interesting that the luminescence decay (Fig. 6b) has a much smaller difference in lifetime (τ_{av} ~ 280 ps); for BIC *J*-aggregates in the TiO_2 matrix (Fig. 6b, curve 1), it is more than twice as large as with that (τ_{av} ~ 120 ps) in water (Fig. 6b, curve 2). For example, adsorption of BIC *J*-aggregates on AAO surface leads to only a small modification in the spectral properties of BIC *J*-aggregates[17], despite a similar positive charge of aluminum oxide pores.

Since there are not enough data to refine the spectral properties of BIC *J*-aggregates in the TiO_2 matrix, we can only assume that they have a modified structure with significant static disorder leading to a very large Stokes shift and a wide luminescence band.

4. Conclusions

In this study, the features of the formation of *J*-aggregates in TiO_2 porous matrices were demonstrated for three cyanine dyes: two cationic PIC and L-21, and anionic BIC. Despite the positive charge of the surface of TiO_2 particles, the best coloration of the matrices was obtained for cationic dyes, while anionic dye BIC is concentrated preferably along the matrix boundaries. For all cases, the aggregation degree was much less compared to solutions with a high contribution of monomeric bands to absorption spectra. A weaker dipole-dipole interaction and a larger static disorder were found for *J*-aggregates in the TiO_2 matrices. The most significant spectral changes were revealed for BIC *J*-aggregates, in contrast to the case of their adsorption on porous aluminum oxide. It can be assumed that sufficiently large pores in the TiO_2 matrix lead to a larger contribution of hydrophobic interaction compared to the Coulomb attraction and capillary effects. When adsorbed in the TiO_2 matrix, L-21 *J*-aggregates demonstrate the best results in terms of the spectral properties. However, the stability of the L-21 *J*-aggregates appears to be very low significantly limiting the possible application of these systems. Thus, the formation of PIC *J*-aggregates in porous matrices formed by TiO_2 microparticles can be considered the best case. For a better understanding of the obtained results on the formation of *J*-aggregates of cyanine dyes, one should compare them with ones for porous matrices formed by TiO_2 nanoparticles.

Acknowledgments. This work was supported by the National Academy of Sciences of Ukraine (project 0117U000989) with partial support from a nominal scholarship of the Verkhovna Rada of Ukraine for Young Scientists — Doctors of Sciences for 2021 (project 0121U112468). The authors thank the Ukrainian Army for the opportunity to prepare the work for publishing. AS expresses sincere gratitude to Dr.Franziska Fennel from the University of Rostock for the invaluable help.

References

1. A.Mishra, R.K.Behera, P.K.Behera et al., *Chem. Rev.*, **100**, 1973 (2000).
2. F.Wurthner, T.E.Kaiser, C.R.Saha-Moller, *Angew. Chemie Int. Ed.*, **50**, 3376 (2011).
3. D.Mobius, *Adv. Mater.*, **7**, 437 (1995).
4. *J*-aggregates, ed. by T.Kobayashi, World Scientific, Singapore (1996).
5. *J*-aggregates, ed. by T.Kobayashi, vol. 2, World Scientific, Singapore (2012).
6. J.L.Bricks, Y.L.Slominskii, I.D.Panas et al., *Methods Appl. Fluoresc.*, **6**, 012001 (2017).
7. A.V.Sorokin, S.L.Yefimova, Y.V.Malyukin, in: Encycl. Polym. Sci. Technol., John Wiley & Sons, Inc., Hoboken, NJ, USA (2018), p.1.
8. H.von Berlepsch, C.Bottcher, A.Ouart et al., *J. Phys. Chem. B*, **104**, 5255 (2000).
9. D.H.Auston, A.A.Ballman, P.Bhattacharya et al., *Appl. Opt.*, **26**, 211 (1987).
10. X.Ma, J.Hua, W.Wu et al., *Tetrahedron*, **64**, 345 (2008).
11. R.Hany, B.Fan, F.A.de Castro et al., *Prog. Photovoltaics Res. Appl.*, **19**, 851 (2011).
12. D.Saccone, S.Galliano, N.Barbero et al., *European J. Org. Chem.*, **2016**, 2244 (2016).
13. S.Jenatsch, L.Wang, N.Leclaire et al., *Org. Electron. Physics. Mater. Appl.*, **48**, 77 (2017).
14. D.Gesevicius, A.Neels, S.Jenatsch et al., *Adv. Sci.*, **5**, 1700496 (2018).
15. A.V.Sorokin, I.Ropakova, I.A.Borovoy et al., *Funct. Mater.*, **24**, (2017).
16. A.V.Sorokin, I.Y.Ropakova, S.Wolter et al., *J. Phys. Chem. C*, **123**, 9428 (2019).
17. A.V.Sorokin, A.V.Voloshko, I.I.Fylymonova et al., *Funct. Mater.*, **21**, 42 (2014).
18. A.V.Sorokin, N.V.Pereverzev, I.I.Grankina et al., *J. Phys. Chem. C*, **119**, 27865 (2015).
19. B.O'Regan, M.Gratzel, *Nature*, **353, 737** (1991).
20. A.Tricoli, A.S.Wallerand, M.Righettoni, *J. Mater. Chem.*, **22**, 14254 (2012).
21. B.O.Aduda, P.Ravirajan, K.L.Choy et al., *Int. J. Photoenergy*, **6**, 141 (2004).
22. M.S.A.Abdel-Mottaleb, M.M.S.Abdel-Mottaleb, H.S.Hafez et al., *Int. J. Photoenergy*, **2014**, 1 (2014).
23. K.Sayama, S.Tsukagoshi, K.Hara et al., *J. Phys. Chem. B*, **106**, 1363 (2002).
24. J.Xiang, C.Chen, Z.Chen et al., *J Colloid Interface Sci*, **254**, 195 (2002).
25. A.Liess, A.Arjona-Esteban, A.Kudzus et al., *Adv. Funct. Mater.*, **29**, 1805058 (2019).
26. S.B.Anantharaman, K.Strassel, M.Diethelm et al., *J. Mater. Chem. C*, **7**, 14639 (2019).
27. I.Renge, U.P.Wild, *J. Phys. Chem. A*, **101**, 7977 (1997).
28. J.R.Lakowicz, Principles of Fluorescence Spectroscopy, 3rd ed., Springer US, Boston, MA (2006).
29. J.Knoester, V.M.Agranovich, in: Thin Film. Nanostructures Electron. Excit. Org. Based Nanostructures, vol. 31, ed. by V.M.Agranovich and G.F.Bassani (2003), p.1.
30. A.V.Sorokin, A.A.Zabolotskii, N.V.Pereverzev et al., *J. Phys. Chem. C*, **119**, 2743 (2015).
31. D.Noukakis, M.Van der Auweraer, F.C.De Schryver, *J. Phys. Chem.*, **98**, 11745 (1994).
32. G.Y.Guralchuk, A.V.Sorokin, I.K.Katrunov et al., *J. Fluoresc.*, **17**, 370 (2007).
33. G.Y.Guralchuk, I.K.Katrunov, R.S.Grynyov et al., *J. Phys. Chem. C*, **112**, 14762 (2008).
34. S.L.Yefimova, G.V.Grygorova, V.K.Klochkov et al., *J. Phys. Chem. C*, **122**, 20996 (2018).
35. A.V.Sorokin, I.Y.Ropakova, R.S.Grynyov et al., *Dye. Pigment.*, **152**, 49 (2018).